Published in final edited form as:
Nat Genet. 2005 May ; 37(5): 526–531.

A genomic screen in yeast implicates kynurenine 3-monooxygenase as a therapeutic target for Huntington's disease

Flaviano Giorgini[1], **Paolo Guidetti**[2], **QuangVu Nguyen**[1], **Simone C. Bennett**[1,3], and **Paul J. Muchowski**[1,4,*]

1*Department of Pharmacology*

4*The Center for Neurogenetics and Neurotherapeutics, University of Washington, Seattle, WA 98195, USA.*

2*Maryland Psychiatric Research Center, University of Maryland School of Medicine, Baltimore, Maryland 21228, USA.*

3*Molecular and Cellular Biology Program, University of Washington School of Medicine, Seattle, Washington 98195, USA.*

Abstract

Huntington's disease (HD) is a fatal neurodegenerative disorder that is caused by an expansion of a polyglutamine (polyQ) tract in the protein huntingtin (Htt)[1], which leads to its aggregation in nuclear and cytoplasmic inclusion bodies[2]. We recently reported the identification of 52 loss-of-function (LOF) mutations in yeast genes that enhance the toxicity of a mutant Htt fragment[3]. Here we report the results from a genome-wide LOF suppressor screen in which 28 gene deletions that suppress toxicity of a mutant Htt fragment were identified. The suppressors are known or predicted to play roles in vesicle transport, vacuolar degradation, transcription, and prion-like aggregation. Among the most potent suppressors identified was Bna4 (kynurenine 3-monooxygenase), an enzyme in the kynurenine pathway of tryptophan degradation that in humans has been linked directly to the pathophysiology of HD by a mechanism that may involve reactive oxygen species[4]. This finding suggests a conserved mechanism of polyQ toxicity from yeast to humans and identifies new candidate therapeutic targets for the treatment of HD.

Similar to what is observed in neurons, expression of a mutant Htt fragment (Htt103Q)[5] in yeast results in the formation of inclusion bodies (IBs) and confers cellular toxicity (Figure 1). We performed a LOF screen with a library of *Saccharomyces cerevisiae* strains to identify gene deletions that suppress Htt103Q-induced toxicity. 28 suppressors out of 4850 strains were identified (Table 1, Figure 1a) that expressed Htt103Q at similar levels to the parental strain (Supplementary Figure 1a). Interestingly, Htt103Q formed IBs in the majority of the LOF suppressor strains (Figure 1b), consistent with previous studies indicating that IB formation by mutant Htt fragments is not sufficient for toxicity, and may instead be a protective mechanism[6,7]. Of the LOF suppressors isolated, ~86% (24/28) correspond to genes with known or predicted functions.

Recent work has implicated the cellular process of autophagy in the pathology of HD[8–10]. Autophagy in yeast occurs in the vacuole, the functional equivalent of the mammalian lysosome. Of the suppressors isolated in our screen with known or predicted functions, 25% (6/24) encode proteins that cluster into the functionally related categories of vesicular transport, vacuolar protein sorting, and vacuolar import (Bfr1, Cyk3, Def1, Mso1, Sna2, Vps53). Since

*To whom correspondence should be addressed. E-mail: mucho@u.washington.edu

many of these gene deletion strains exhibit perturbation of protein sorting to the vacuole, we hypothesize that abnormal sorting of Htt103Q relieves toxicity.

A large body of evidence indicates that transcriptional dysregulation may play an important role in HD pathogenesis[11], and it is not surprising that ~25% (6/24) of the suppressors identified in our screen encode proteins that are involved directly in transcription or in establishment/maintenance of chromatin architecture (Mbf1, Nhp6b, Paf1, Rxt3, Ume1, Ylr278c). Two of these proteins, Ume1 and Rxt3, are members of the yeast Rpd3 histone deacetylase (HDAC) complex. Pharmacological and genetic inhibition of the functionally equivalent HDAC complex in *Drosophila* ameliorates neurodegeneration and viability in polyQ disease models[12], while pharmacological inhibition of HDAC activity improves motor deficits in a mouse HD model[13,14]. Provocatively, Ume1 is required for full transcriptional repression of a subset of genes in yeast, in a mechanism requiring Rpd3 (ref. 15), suggesting that genetic inhibition of the yeast Rpd3 HDAC complex relieves polyQ toxicity in a mechanism similar to that observed in fly and mouse polyQ disease models. The simplest interpretation of these results is that putative transcriptional abnormalities induced by Htt103Q are correlated to toxicity, and that transcriptional dysfunction is ameliorated by the suppressor mutations.

Approximately 21% (5/24) of the suppressor genes encode known yeast prions (Rnq1) or proteins containing Q/N-rich regions that may mediate prion-like aggregation (Def1, Ybr016w, Yir003w, Ylr278c)[16]. Rnq1 in its prion conformation is necessary for Htt103Q-mediated toxicity[5] and, importantly, analysis of several of the suppressor strains confirmed that Rnq1 remains in its prion conformation when expression of Htt103Q was induced (Supplementary Figure 1b). The finding that a network of putative prion-like proteins is required for Htt103Q-mediated toxicity in yeast is novel, and suggests that yeast prions may have evolved to modulate aggregation and/or the biological functions of Q/N-rich proteins.

Among the most potent LOF suppressor mutations identified in our screen was a gene that encodes Bna4 [kynurenine 3-monooxygenase (KMO)]. This mitochondrial enzyme is particularly intriguing because it functions in the kynurenine pathway, which is activated in HD patients and in animal models of HD[4]. The kynurenine pathway is the major route of tryptophan degradation in eukaryotes, and leads to synthesis of NAD^+ (Figure 2a). Intrastriatal injection of the kynurenine pathway metabolite quinolinic acid (QUIN) in rodents reproduces behavioral and pathological features of HD[17], raising the possibility that alterations in QUIN metabolism may be central to HD pathophysiology[4]. The endogenous levels of QUIN, which is synthesized via the cerebral kynurenine pathway, are elevated in the neostriatum and in the cortex of early stage (grade 0 and 1) HD patients[18]. This pathway also includes 3-hydroxykynurenine (3HK) which potentiates QUIN neurotoxicity[19] and is elevated preferentially in the neostriatum and cortex of stage 1 HD patients and in mice expressing mutant Htt[20]. It is thus intriguing that deletion of *BNA4*, predicted to eliminate production of both 3HK and QUIN in yeast, strongly suppressed Htt103Q-mediated toxicity (Figure 2b).

The enzymes and metabolites involved in the kynurenine pathway are remarkably well conserved between yeast and humans (Figure 2a), which led us to assay cell viability of gene deletion strains for all of the enzymes involved in this pathway when expressing Htt103Q (Figure 2b). In addition, we characterized levels of 3HK and QUIN in several of these strains. As predicted from studies in humans and mice, 3HK levels increased ~2.2-fold in yeast cells that express Htt103Q versus cells expressing Htt25Q ($P = 0.019$) or empty vector control ($P < 0.001$) (Figure 3a). Levels of QUIN were also increased significantly ($P < 0.001$) in cells that express Htt103Q (Figure 3a). As predicted, no 3HK or QUIN was detected in cells lacking Bna4 (Figure 3a).

The enzyme encoded by *BNA1*, 3-hydroxyanthranilate 3,4-dioxygenase, functions downstream of KMO and catalyzes the final enzyme-dependent step of the kynurenine pathway upstream of QUIN (Figure 2a). Therefore, deletion of *BNA1* is predicted to eliminate production of QUIN, while causing increased levels of 3HK. Indeed, levels of 3HK were increased significantly in *bna1*Δ cells expressing Htt103Q as compared to either the parental strain or *bna1*Δ carrying empty vector ($P < 0.001$ and $P < 0.01$, respectively), while QUIN levels were undetectable (Figure 3a). Deletion of *BNA1* partially suppressed Htt103Q-mediated toxicity (Figure 2b), consistent with an additive effect of QUIN and 3HK in Htt103Q-mediated toxicity.

Deletion of two kynurenine pathway genes, *ARO9* and *NPT1*, enhanced Htt103Q toxicity (Figure 2b). Deletion of *ARO9* blocks synthesis of kynurenic acid from kynurenine, likely increasing levels of kynurenine and downstream metabolites. In addition, kynurenic acid may be protective, due to its activity as a free-radical scavenger[21]. Deletion of *NPT1* blocks synthesis of NAD^+ from nicotinic acid, forcing all synthesis of NAD^+ to occur via the kynurenine pathway, and likely causing upregulation of the pathway. Consistent with the enhancement of Htt-103Q toxicity observed in *aro9*Δ and *npt1*Δ cells, levels of 3HK were increased 90 and 15-fold ($P < 0.001$), respectively, and QUIN was elevated 10-fold in *npt1*Δ cells ($P < 0.001$) in comparison to the parental strain that expressed Htt-103Q (Figure 3b). While levels of 3HK were also elevated in *aro9*Δ carrying empty vector as compared to the parental strain, expression of Htt103Q increased levels of 3HK over 40-fold ($P < 0.001$) (Figure 3b). The remaining kynurenine pathway gene deletions did not have a detectable effect upon Htt103Q-mediated toxicity.

Ro 61-8048, a high-affinity small molecule inhibitor of KMO (the mammalian ortholog of *BNA4*)[22] is neuroprotective in models of brain ischemia[23] and in a genetic model of paroxysmal dyskinesia[24]. We next explored if pharmacological inhibition of Bna4 by Ro 61-8048 could reduce levels of 3HK and QUIN in yeast and thereby suppress Htt103Q-dependent toxicity. Treatment of yeast cells expressing Htt103Q with Ro 61-8048 reduced levels of 3HK to nearly wild-type levels (Figure 3c). However, levels of the downstream metabolite QUIN were unaffected by Ro 61-8048 treatment, indicating that Ro 61-8048 only partially inhibits Bna4 activity in yeast. Consistent with this result, treatment of yeast cells that express Htt103Q with Ro 61-8048 conferred a partial, but significant, improvement in growth that was dose-dependent (Figure 3d).

How might kynurenines induce toxicity in cells that express a mutant Htt? The neurotoxin 3HK is present in the brain in nanomolar concentrations, but at higher levels can kill neurons by generating toxic free radicals that initiate a cascade of events leading to cell death[25]. Toxicity of QUIN, on the other hand, is proposed to be due to a combination of factors: activation of N-methyl-D-aspartate (NMDA) receptors and generation of toxic free radicals[25]. The common feature of 3HK and QUIN to generate toxic free radicals led us to analyze levels of reactive oxygen species (ROS) by fluorescence microscopy in yeast cells in the absence and presence of Htt103Q (Figure 4a). An ~8-fold increase in ROS ($P = 0.001$) was detected in cells that express Htt103Q when compared to control cells that express Htt25Q, while ROS levels in *bna4*Δ cells that express Htt103Q were not statistically different than those observed with Htt25Q ($P = 0.4$) (Figure 4a and 4b). In addition, Ro 61-8048 treatment of cells expressing Htt103Q reduced levels of ROS significantly ($P = 0.011$) (Figure 4c). Together this data shows that genetic or pharmacological reduction of KMO activity ameliorates increases of ROS in yeast expressing Htt103Q. This supports observations in neuronal cells and mice showing increases in ROS with expression of mutant Htt[26,27], and suggests that increased ROS levels in yeast cells that express Htt103Q are likely due to abnormally high levels of 3HK and QUIN.

The results presented in this study suggest that a conserved mechanism of polyQ toxicity exists in yeast and HD patients involving upregulation of the kynurenine pathway metabolites 3HK

and QUIN leading to generation of ROS. Since it is known that the majority of brain kynurenines are synthesized in astrocytes and microglia[25] and that microglia are activated in HD patients[28] and by intrastriatal QUIN injection in rats[29], our results suggest that some of the effects of mutant Htt may not be cell-autonomous and may involve cell types in addition to neurons. It has been proposed previously that secretion of cytokines by dysfunctional neurons expressing mutant Htt leads to the local activation of microglia, causing 3HK and QUIN production, and that this in turn contributes to neurodegeneration observed in HD[25]. In an alternative, but not non-mutually exclusive model, we propose here that expression of mutant Htt in astrocytes and microglia leads directly to cellular dysfunction in these cells, thereby resulting in elevated 3HK and QUIN production (Figure 5).

Inhibition of the kynurenine pathway by genetic or pharmacological means has a significant effect on polyQ-mediated toxicity, 3HK and QUIN production, and generation of ROS in yeast expressing Htt103Q. A recent high-throughput screen of 16,000 small chemical compounds in yeast expressing Htt103 led to the identification of a single drug that suppressed neurodegeneration in a fly polyQ model[30]. Provacatively, this compound is a structural analog of the KMO inhibitor Ro 61-8048, providing further support that pharmacological inhibition of KMO may ameliorate mutant Htt-mediated toxicity. Our data suggests that KMO, and perhaps other enzymes of the kynurenine pathway, are excellent candidates for drug development for HD. Pre-clinical trials with Ro 61-8048 are currently underway using HD mouse models. Finally, the results from this and our previous genetic screen[3] may help guide future efforts in cellular and animal models to elucidate the genetic pathways and molecular mechanisms underlying neurodegeneration in HD.

Methods

Yeast genomic screen for LOF suppressors of Htt103Q-mediated toxicity

The yeast gene deletion set (YGDS), a collection of 4850 yeast MATa (BY4741) haploid deletion strains, was obtained frozen in glycerol stocks in 96-well microtiter dishes from Research Genetics (Huntsville, AL). These strains were grouped into 4 pools of approximately 1200 strains, as previously described[3]. The deletion set was transformed with pYES2-Htt103Q-GFP[5] using the lithium acetate method. Htt103Q is a galactose (GAL)-inducible, FLAG- and GFP-tagged construct encoding the first 17 amino acids of Htt fused to a polyQ tract of 103 glutamines, a length beyond the pathogenic threshold for HD. Each pool was screened to ~12-fold coverage via selection on plates containing synthetic complete media lacking uracil (SC −Ura) for a combined total of ~6.0×10^4 individual transformants. The total number of transformants was estimated on a control plate containing glucose (GLU) as the sole carbon source (SC −Ura +GLU). Loss-of-function suppressors of Htt103Q toxicity were selected on plates containing GAL as the sole carbon source (SC −Ura +GAL). Presence of GAL induces the expression of Htt103Q via the *GAL1* promoter. Plates were analyzed after 3 days of incubation at 30 °C, and colonies that grew on the SC −Ura +GAL plates were selected for further analysis. 366 colonies underwent preliminary retesting by being streaked onto a master plate containing SC −Ura +GAL. Transformants that retained the ability to grow on plates containing GAL were selected for further testing.

Identification and retesting of suppressors

Colony PCR analysis was used to amplify a 20 base pair barcode sequence that uniquely identified each deletion strain for all of the 366 suppressors isolated in the screen. The PCR product was sequenced using standard DNA sequencing methods, and the barcode sequence was used as a query in a blast search of the yeast gene deletion set database (*Saccharomyces* Genome Database, Stanford University), revealing the identity of the deletion strain. Since many gene deletions were isolated numerous times, the 366 suppressors defined a total of 167

individual gene deletions. All identified suppressor strains were streaked out fresh from the original frozen stocks of the YGDS, and retransformed with the pYES2-Htt103Q construct for subsequent analysis. All transformed deletion strains were re-tested for suppression of Htt103Q-mediated toxicity using spotting assays, to ensure that suppression of toxicity was not due to second-site mutations. We did not observe any strong growth defects among the strains being tested that might have affected interpretation of the suppression analysis. ~18% (30/167) of the putative suppressors retested for suppression of toxicity and were kept for further analysis. Mammalian homologs of yeast genes were determined using annotations from the Incyte Proteome BioKnowledge Library. In the proteome library, protein sequences are aligned with Gapped BLAST (v2.0.10) with SEG and COIL filtering; alignments with an expectation score of less than or equal to 1×10^{-3} are refined by Smith-Waterman alignment algorithms from the USC Sequence alignment package v2.0, with no filtering. In this study, homologs for yeast proteins without known functional orthologs were determined by selection from related proteins with an expectation score of 1×10^{-4} or smaller and match lengths of >50% of the full length sequence of the homologous protein. Brain expression data based upon cDNA expression profiles at Unigene database.

Microscopy

Fluorescent images were acquired using a Deltavision deconvolution microscope with 40x or 100x oil immersion objectives. 1-2 ml yeast cultures were grown to log phase (OD_{600} 0.5-0.9) in SC−Ura +GAL or SC−Ura +GLU media for 2 days. The cultures were centrifuged at 10,000g for 2 minutes, the media was removed, and the pellet was resuspended in 100 μl PBS. 1 μl of the resuspension was pipetted onto a pad of 5% agarose on a microscope slide and sealed with a cover slip. For the examination of fluorescence by GFP, cells were exposed to light of wavelength 490 nm and viewed through a 528 +/− 38 nm filter. For examination of ROS using DHE (Molecular Probes, Eugene, OR), yeast were grown to log phase in 1-2 ml cultures in SC −Ura +GAL or SC−Ura +GLU media. DHE is oxidized to ethidium by superoxide anions, and thus the production of ROS is visualized by an increase in ethidium staining of DNA. Cultures were centrifuged at 10,000g for 2 minutes followed by resuspension in 100 μl PBS. DHE was added at a concentration of 5uM, and the cells were incubated with shaking for 30 minutes at 30° C. The cells were centrifuged, the media was removed, and the pellet was resuspended in 100 μl PBS. 1 μl of cells was added to a microscope slide with a 5% agarose pad. Quantification of ROS was performed using the dye DHR (Molecular Probes, Eugene, OR). DHR passively diffuses across cell membranes where it is oxidized to cationic rhodamine 123. For visualization of DHR, we exposed cells to light of wavelength 555nm and viewed through a 617 +/− 73 nm filter. Experiments were done in triplicate with cell counts of ~300 cells per sample. Experiments with DHR were performed using Htt25Q and Htt103Q tagged with RFP. Ro 61-8048 treatment was done in the pleiotropic drug response deletion strain *pdr1*δ*pdr3*Δ in the W303 strain background. The no drug control was done with 1% DMSO. All images were acquired and deconvolved using Softworx (Applied Precision, Issaquah, WA) with an Olympus 1X-HLS100 camera.

Biochemical Analysis

Yeast extracts were prepared as described above, except ultrapure water was substituted for lysis. 6% perchloric acid was added at a ratio of 1:5 and precipitated protein was separated by centrifugation. Levels of both 3HK and QUIN were determined from the same yeast extracts in triplicate using HPLC and GC/MS analyses as described previously[18].

Growth Curves

Growth curves were initiated by diluting overnight SC −Ura raffinose cultures to OD_{600} 0.2, at which Htt103Q expression was induced with the addition of a final concentration of 2%

GAL. Optical density was measured at OD_{600} on an Ultrospec 2100 Pro spectrophotometer over a period of 16.5 hours. Addition of drug (Ro 61-8048, 1 μM or 100 μM in 1% DMSO) or 1% DMSO to the appropriate samples was done coincidentally with GAL induction. Drug testing was done in the drug permeable strain *erg6*Δ in the BY4741 parental background.

Supplementary Material

Refer to Web version on PubMed Central for supplementary material.

Acknowledgements

P.J.M. is supported by the National Institute of Neurological Disease and Stroke, by an NIH construction award, by the Alzheimer's Disease Research Center at the University of Washington, and by the Hereditary Disease Foundation under the auspices of the “Cure Huntington's Disease Initiative”. F.G. is supported by a post-doctoral fellowship from the HighQ foundation. We thank M. Sherman for the pYES2-Htt25Q and pYES2-Htt103Q plasmids and S. Lindquist for the RNQ antibody and the *pdr1*Δ*pdr3*Δ drug testing strain. Ro 61-8048 was generated and kindly provided by W. Frostl, Novartis, Switzerland. Finally, the authors thank R. Schwarcz for enthusiastic discussions about our data and advice regarding this project and K. Neireiter for his wonderful illustration.

Literature Cited

1. A novel gene containing a trinucleotide repeat that is expanded and unstable on Huntington's disease chromosomes. The Huntington's Disease Collaborative Research Group. Cell 1993;72:971–983. [PubMed: 8458085]
2. Scherzinger E, et al. Huntingtin-encoded polyglutamine expansions form amyloid-like protein aggregates in vitro and in vivo. Cell 1997;90:549–558. [PubMed: 9267034]
3. Willingham S, Outeiro TF, DeVit MJ, Lindquist SL, Muchowski PJ. Yeast genes that enhance the toxicity of a mutant huntingtin fragment or alpha-synuclein. Science 2003;302:1769–1772. [PubMed: 14657499]
4. Schwarcz R. The kynurenine pathway of tryptophan degradation as a drug target. Curr Opin Pharmacol 2004;4:12–17. [PubMed: 15018833]
5. Meriin AB, et al. Huntington toxicity in yeast model depends on polyglutamine aggregation mediated by a prion-like protein Rnq1. J Cell Biol 2002;157:997–1004. [PubMed: 12058016]
6. Muchowski PJ, Ning K, D'Souza-Schorey C, Fields S. Requirement of an intact microtubule cytoskeleton for aggregation and inclusion body formation by a mutant huntingtin fragment. Proc Natl Acad Sci U S A 2002;99:727–732. [PubMed: 11792857]
7. Arrasate M, Mitra S, Schweitzer ES, Segal MR, Finkbeiner S. Inclusion body formation reduces levels of mutant huntingtin and the risk of neuronal death. Nature 2004;431:805–810. [PubMed: 15483602]
8. Ravikumar B, Duden R, Rubinsztein DC. Aggregate-prone proteins with polyglutamine and polyalanine expansions are degraded by autophagy. Hum Mol Genet 2002;11:1107–1117. [PubMed: 11978769]
9. Qin ZH, et al. Autophagy regulates the processing of amino terminal huntingtin fragments. Hum Mol Genet 2003;12:3231–3244. [PubMed: 14570716]
10. Ravikumar B, et al. Inhibition of mTOR induces autophagy and reduces toxicity of polyglutamine expansions in fly and mouse models of Huntington disease. Nat Genet 2004;36:585–595. [PubMed: 15146184]
11. Sugars KL, Rubinsztein DC. Transcriptional abnormalities in Huntington disease. Trends Genet 2003;19:233–238. [PubMed: 12711212]
12. Steffan JS, et al. Histone deacetylase inhibitors arrest polyglutamine-dependent neurodegeneration in Drosophila. Nature 2001;413:739–743. [PubMed: 11607033]
13. Hockly E, et al. Suberoylanilide hydroxamic acid, a histone deacetylase inhibitor, ameliorates motor deficits in a mouse model of Huntington's disease. Proc Natl Acad Sci U S A 2003;100:2041–2046. [PubMed: 12576549]
14. Ferrante RJ, et al. Histone deacetylase inhibition by sodium butyrate chemotherapy ameliorates the neurodegenerative phenotype in Huntington's disease mice. J Neurosci 2003;23:9418–9427. [PubMed: 14561870]

15. Mallory MJ, Strich R. Ume1p represses meiotic gene transcription in Saccharomyces cerevisiae through interaction with the histone deacetylase Rpd3p. J Biol Chem 2003;278:44727–44734. [PubMed: 12954623]

16. Michelitsch MD, Weissman JS. A census of glutamine/asparagine-rich regions: implications for their conserved function and the prediction of novel prions. Proc Natl Acad Sci U S A 2000;97:11910–11915. [PubMed: 11050225]

17. Schwarcz R, Whetsell WO Jr. Mangano RM. Quinolinic acid: an endogenous metabolite that produces axon-sparing lesions in rat brain. Science 1983;219:316–318. [PubMed: 6849138]

18. Guidetti P, Luthi-Carter RE, Augood SJ, Schwarcz R. Neostriatal and cortical quinolinate levels are increased in early grade Huntington's disease. Neurobiol Dis 2004;17:455–461. [PubMed: 15571981]

19. Guidetti P, Schwarcz R. 3-Hydroxykynurenine potentiates quinolinate but not NMDA toxicity in the rat striatum. Eur J Neurosci 1999;11:3857–3863. [PubMed: 10583474]

20. Guidetti P, Reddy PH, Tagle DA, Schwarcz R. Early kynurenergic impairment in Huntington's disease and in a transgenic animal model. Neurosci Lett 2000;283:233–235. [PubMed: 10754231]

21. Goda K, Hamane Y, Kishimoto R, Ogishi Y. Radical scavenging properties of tryptophan metabolites. Estimation of their radical reactivity. Adv Exp Med Biol 1999;467:397–402. [PubMed: 10721081]

22. Rover S, Cesura AM, Huguenin P, Kettler R, Szente A. Synthesis and biochemical evaluation of N-(4-phenylthiazol-2-yl)benzenesulfonamides as high-affinity inhibitors of kynurenine 3-hydroxylase. J Med Chem 1997;40:4378–4385. [PubMed: 9435907]

23. Moroni F, Cozzi A, Peruginelli F, Carpenedo R, Pellegrini-Giampietro DE. Neuroprotective effects of kynurenine-3-hydroxylase inhibitors in models of brain ischemia. Adv Exp Med Biol 1999;467:199–206. [PubMed: 10721057]

24. Richter A, Hamann M. The kynurenine 3-hydroxylase inhibitor Ro 61-8048 improves dystonia in a genetic model of paroxysmal dyskinesia. Eur J Pharmacol 2003;478:47–52. [PubMed: 14555184]

25. Schwarcz R, Pellicciari R. Manipulation of brain kynurenines: glial targets, neuronal effects, and clinical opportunities. J Pharmacol Exp Ther 2002;303:1–10. [PubMed: 12235226]

26. Wyttenbach A, et al. Heat shock protein 27 prevents cellular polyglutamine toxicity and suppresses the increase of reactive oxygen species caused by huntingtin. Hum Mol Genet 2002;11:1137–1151. [PubMed: 11978772]

27. Perez-Severiano F, et al. Increased formation of reactive oxygen species, but no changes in glutathione peroxidase activity, in striata of mice transgenic for the Huntington's disease mutation. Neurochem Res 2004;29:729–733. [PubMed: 15098934]

28. Sapp E, et al. Early and progressive accumulation of reactive microglia in the Huntington disease brain. J Neuropathol Exp Neurol 2001;60:161–172. [PubMed: 11273004]

29. Ryu JK, Kim SU, McLarnon JG. Blockade of quinolinic acid-induced neurotoxicity by pyruvate is associated with inhibition of glial activation in a model of Huntington's disease. Exp Neurol 2004;187:150–159. [PubMed: 15081596]

30. Zhang X, et al. A potent small molecule inhibits polyglutamine aggregation in Huntington's disease neurons and suppresses neurodegeneration in vivo. Proc Natl Acad Sci U S A 2005;102:892–897. [PubMed: 15642944]

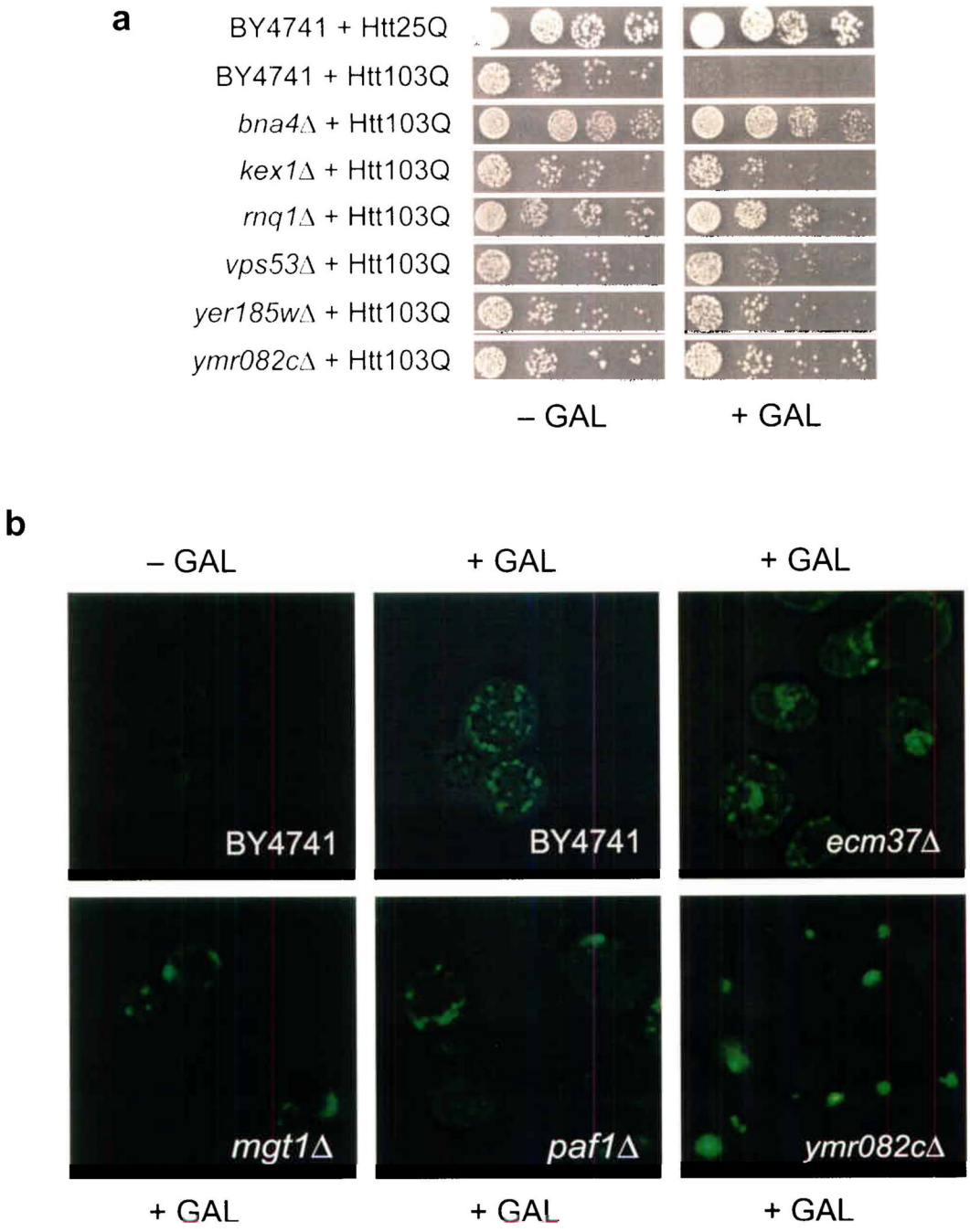

Figure 1.

Suppression of Htt103Q toxicity in yeast gene deletion strains. **a**, Cell viability (spotting) assays are shown for the library parental strain, BY4741, and 6 gene deletion strains that suppress Htt103Q-mediated toxicity. Shown are five-fold serial dilutions starting with equal numbers of cells. Growth on media containing GAL induces expression of Htt103Q. **b**, Fluorescence microscopy of the localization of Htt103Q in IBs (GFP labeling in green). A large number of small IBs form in the parental yeast strain (BY4741) expressing Htt103Q-GFP under inducing conditions (+GAL). The majority of suppressor strains also contained Htt103Q IB's under inducing conditions. A sampling of these includes *ecm37*Δ, *mgt1*Δ, *paf1*Δ, and *ymr082c*Δ.

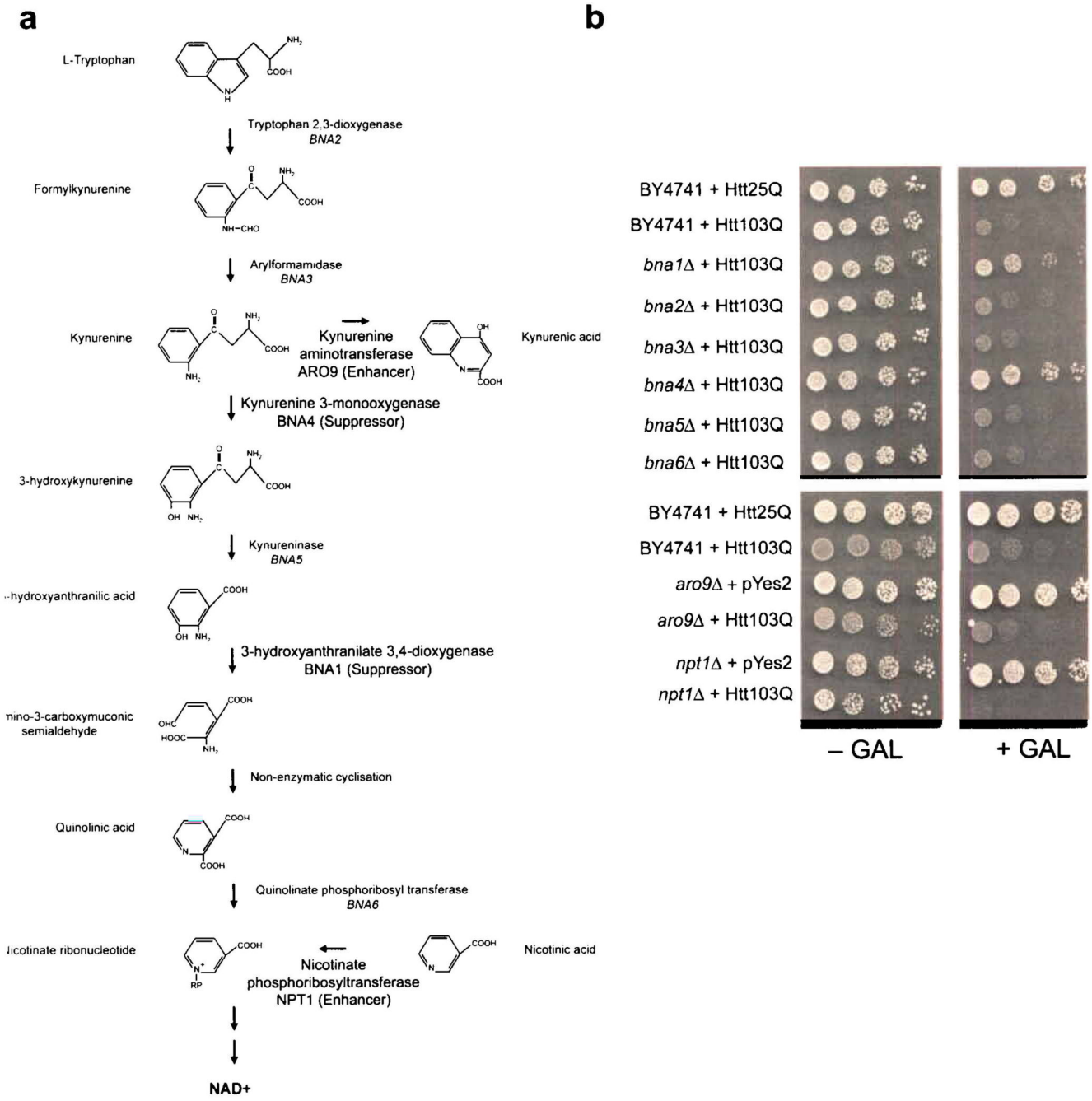

Figure 2.

Genetic analysis of the kynurenine pathway on Htt103Q-mediated toxicity. **a**, Schematic representation of the kynurenine pathway in yeast and mammals. Arrows represent enzymatic steps in the pathway, with the respective enzymes listed to the right. The yeast genes encoding the enzymes are listed below each respective enzyme. Gene deletions that enhance or suppress toxicity of Htt103Q are noted with bold italics. **b**, Analysis of Htt103Q toxicity by cell viability (spotting assays) in the parental yeast strain (BY4741) and the kynurenine pathway gene deletion strains. pYES2 is the empty vector control. Shown are five-fold serial dilutions starting with equal numbers of cells. Growth on media containing GAL induces expression of the Htt103Q.

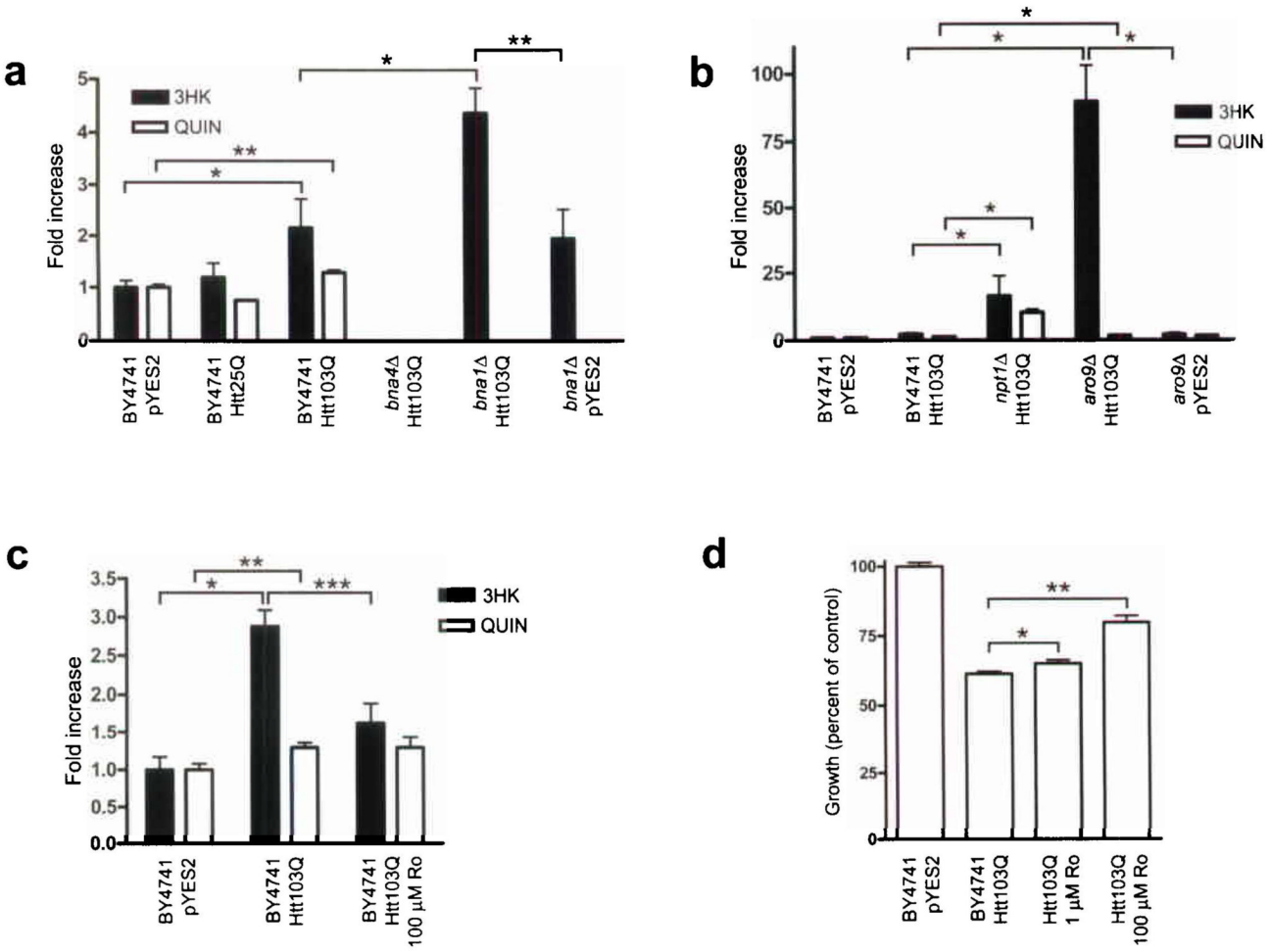

Figure 3.

Htt103Q toxicity is mediated in part by 3HK and QUIN. **a**, Changes in levels of 3HK and QUIN in parental, *bna1*Δ, and *bna4*Δ cells expressing Htt103Q (*$P < 0.001$, **$P < 0.01$). **b**, Changes in 3HK and QUIN levels in *aro9*Δ and *npt1*Δ strains expressing Htt103Q (*$P < 0.001$). **c**, 3HK and QUIN levels with Ro 61-8048 treatment (*$P < 0.001$, **$P = 0.003$, ***$P < 0.01$) **d**, Growth with Ro 61–8048 treatment; 1 μM (** $P = 0.015$) and 100 μM (**$P < 0.001$). All statistical comparisons were performed using Student's *t*-test.

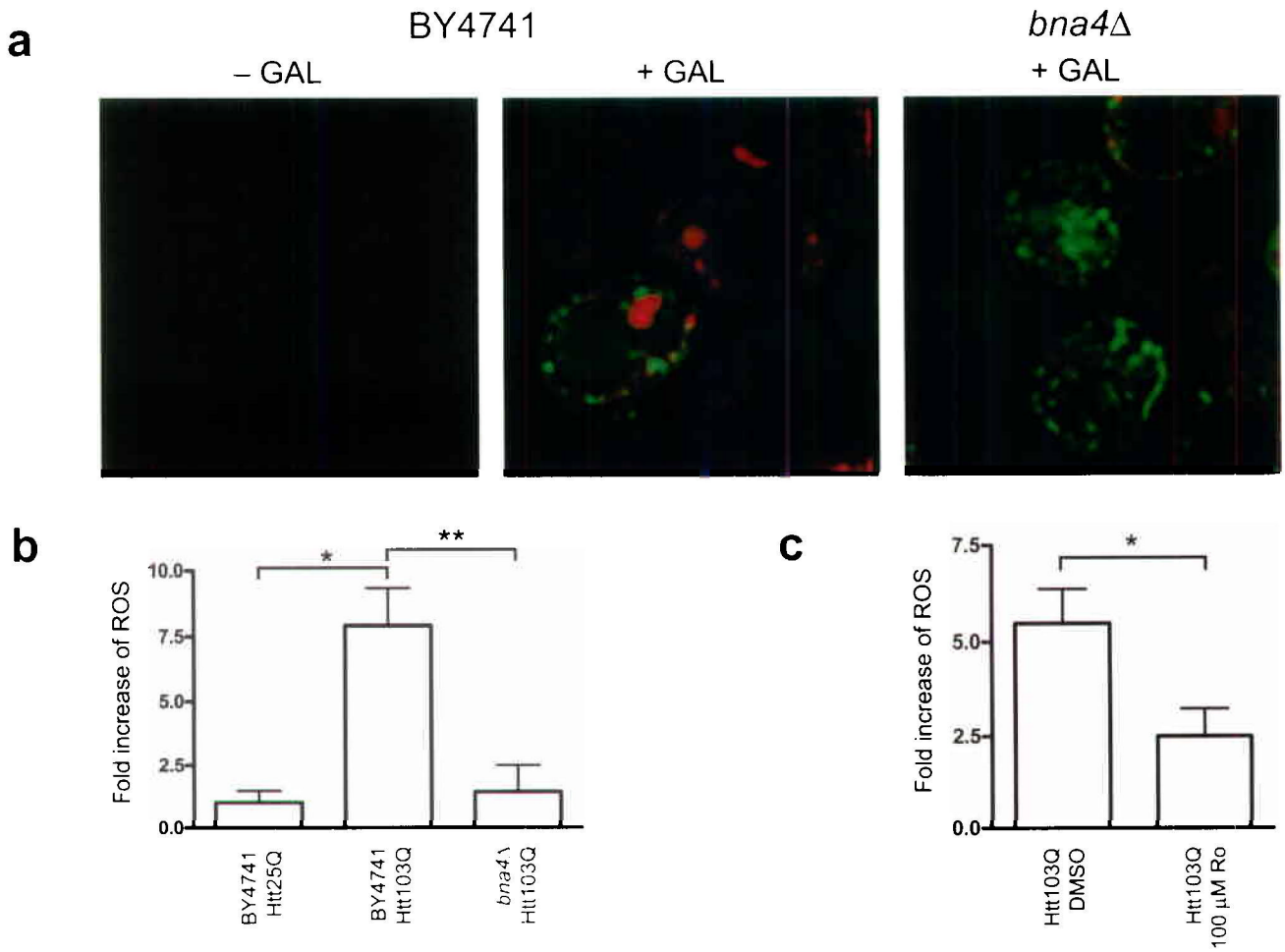

Figure 4.

Htt103Q toxicity is mediated in a manner that involves ROS. **a**, ROS is visualized as red fluorescence while Htt103Q aggregates were visualized by GFP fluorescence. Parental cells expressing Htt103Q showed high levels of ROS, while in *bna4*Δ cells expressing Htt103Q ROS are not detected. **b**, Changes in levels of ROS (**P* = 0.001, ***P* = 0.002). **c**, Ro 61-8048 decreases levels of ROS in cells expressing Htt103Q (**P* = 0.011). All statistical comparisons were performed using Student's *t*-test.

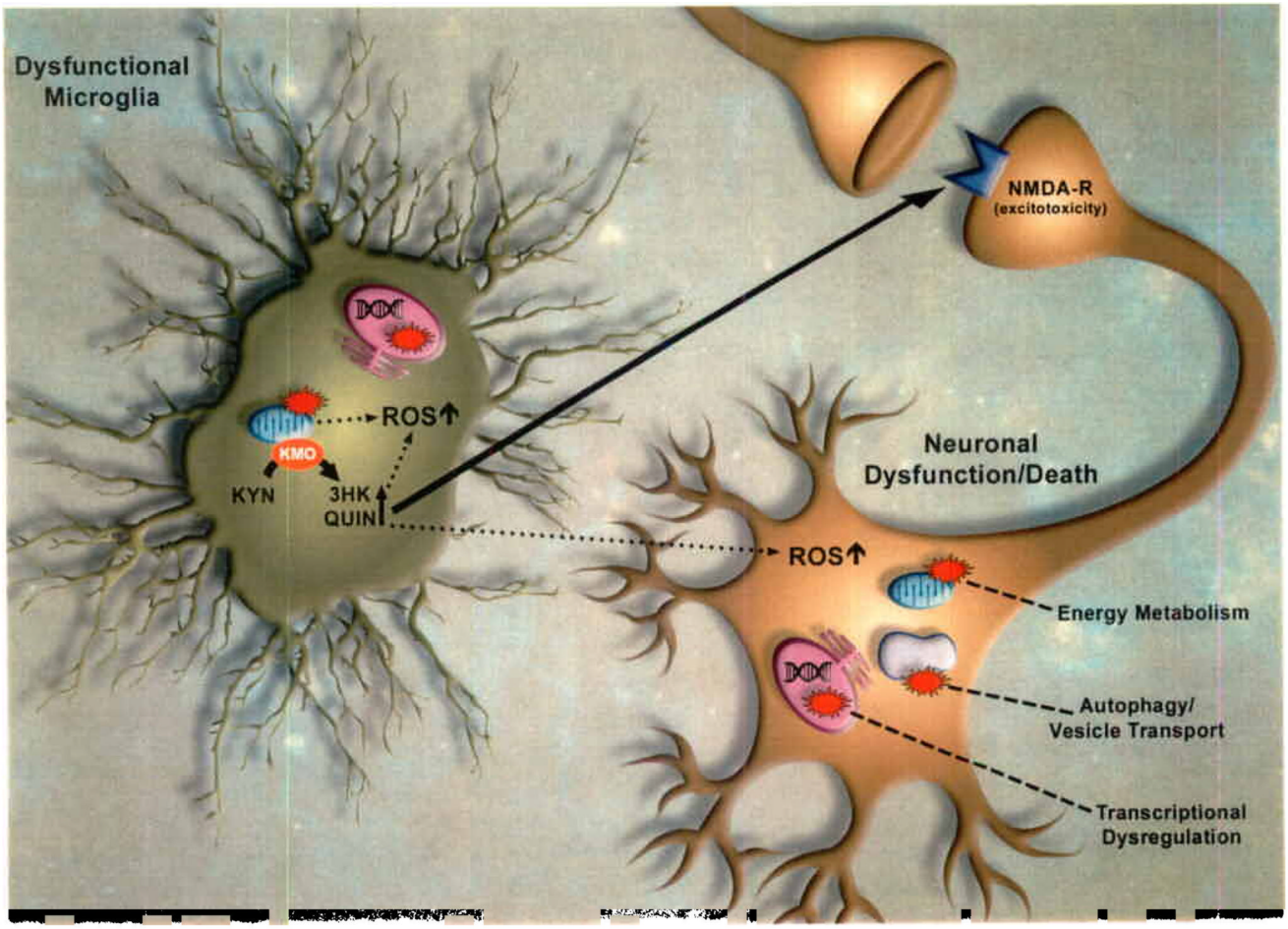

Figure 5.

Model depicting the non-cell autonomous contribution by microglia to neuronal dysfunction in Huntington's disease (HD). In this model, cell-autonomous expression of mutant Htt in microglia causes dysfunction, perhaps by interactions with mitochondria or the mitochondrial membrane protein KMO, leading to upregulation of 3HK and QUIN synthesis, and thereby increased levels of ROS. The combined effects of ROS and NMDA receptor-mediated excitotoxicity by QUIN contribute to the dysfunction of neurons expressing mutant Htt. Other functional categories represented in our genomic screen, and previously implicated in HD, are highlighted in the dysfunctional neuron.

Table 1

Yeast strains that suppress Htt103Q-mediated toxicity.

Strain	Homolog	Function
Vesicular transport, vacuolar protein sorting, and vacuolar import		
*bfr1*Δ	No	mRNA metabolism; defects in vacuolar targeting
*cyk3*Δ	No	Cytokinesis; defective in vacuolar targeting
*def1*Δ	Yes	Involved in vacuolar import; putative prion
*mso1*Δ	No	Component of secretory vesicle docking complex
*sna2*Δ	No	Protein-vacuolar targeting
*vps53*Δ	Yes*	Protein sorting in late golgi
Transcription or establishment/maintenance of chromatin architecture		
*mbf1*Δ	Yes*	Transcription from Pol II promoter
*nhp6b*Δ	Yes*	Transcription from Pol III promoter
*paf1*Δ	Yes*	Transcription initiation from a Pol II promoter
*rxt3*Δ	No	Member of Rpd3 histone deacetylase C (HDAC) complex
*ume1*Δ	Yes*	Transcriptional repressor of Rpd3 HDAC complex
*yir278c*Δ	No	Transcription from Pol II promoter; putative prion
Known and putative yeast prion genes		
*def1*Δ	Yes	Involved in vacuolar import; putative prion
*mq1*Δ	Yes	Required for resistance to certain drugs; yeast prion
*ybr016w*Δ	No	Putative prion
*yir003w*Δ	Yes*	Member of the F-actin capping protein complex; putative prion
*yir278c*Δ	No	Transcription from Pol II promoter; putative prion
Other cellular processes		
*arg7*Δ	No	Omithine acetyltransferase; arginine biosynthesis
*bna4*Δ	Yes*	Kynurenine 3-monooxygenase; NAD* synthesis
*ecm37*Δ	No	Possibly involved in cell wall structure
*hsp104*Δ	Yes*	Heat shock protein; response to oxidative stress
*mgt1*Δ	Yes*	O6-methylguanine DNA repair methyltransferase
*pho87*Δ	Yes*	Inorganic phosphate transporter activity
*rdh54*Δ	Yes*	Required for mitotic diploid-specific recombination and meiosis
*ydr287w*Δ	Yes*	Inositol monophosphatase; phospholipid metabolism
*yer185w*Δ	No	Response to toxin
Genes with unknown function		
*smy2*Δ	No	Unknown
*yir454w*Δ	No	Unknown
*ymr082c*Δ	No	Unknown
*ymr244c-a*Δ	Yes*	Unknown

The homolog category indicates yeast genes with known mammalian homologs. Homology was determined using annotations from the Incyte Proteome BioKnowledge Library. See Materials and Methods for further details.

*Homologs known to be expressed in the brain.